To begin to understand the nano motors responsible for bacterial motility, we first must consider the remarkable different environment that a bacteria experiences. One in which viscosity dominates over inertial forces, described by the dimension-less parameter, the Reynolds number.

The Reynolds number is defined as the ratio of inertial forces to viscous forces:

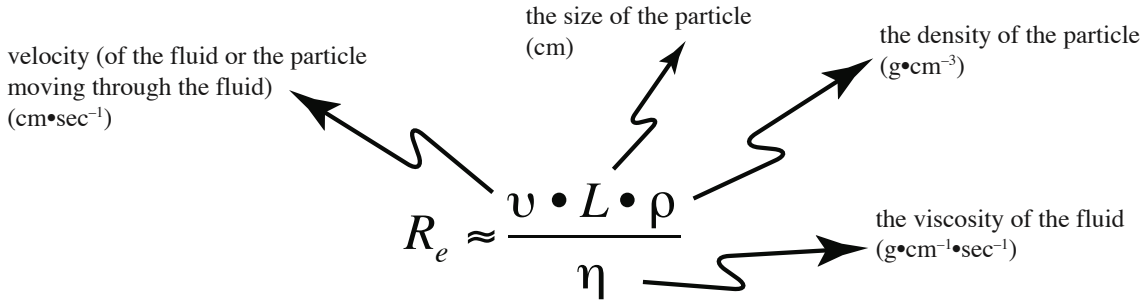

There are three characteristic Reynolds number environments[1], when it is less than 1, greater than 1 but less than 10^5, and when it is greater than 10^6.

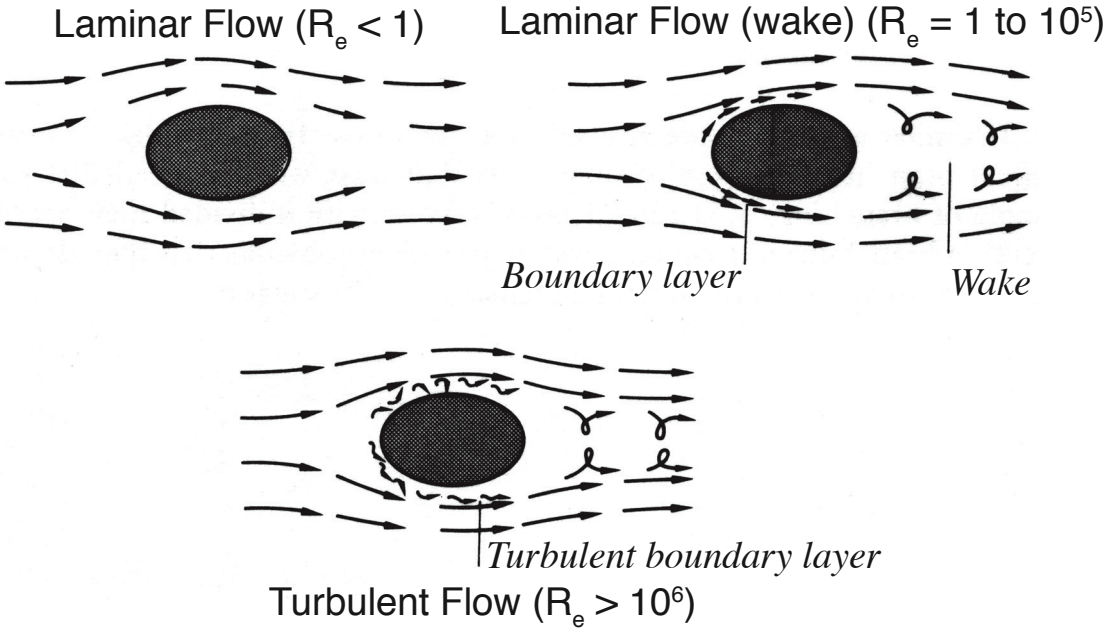

While some organisms may achieve high Reynolds number (fast swimming fish, for example), with its small size and relatively low velocities, a bacteria has a very small-Reynolds number, about 10^{-4} or so. Thus, viscosity dominates.

[1]Source: Alexander, R. McNeill (1971) Size and Shape. Edward Arnold Ltd. pp. 34–42.

$$R_e \approx \frac{\upsilon \bullet L \bullet \rho}{\eta}$$

units : $\dfrac{\text{cm sec}^{-1} \bullet \text{ cm} \bullet \text{ gm cm}^{-3}}{\text{gm cm}^{-1} \text{ sec}^{-1}}$

$\dfrac{\text{gm cm}^{-1} \text{ sec}^{-1}}{\text{gm cm}^{-1} \text{ sec}^{-1}}$

To engineers and biologists, the description of the Reynolds number as the ratio of inertial forces to viscous forces is simple and straightforward, but a physicist would wonder how this could be, since forces (F=m•a), either inertial or viscous, seem to be absent from the Reynolds Number equation. The following is a somewhat rigorous derivation of the Reynolds Number, to explain how the ratio of inertial to viscous forces simplifies to the Reynolds equation[1]. Consider fluid flow around a spherical object:

To move around the spherical object, the volume element has to accelerate to change direction during the encounter (the time will be approximately the radius of the object divided by the velocity of fluid flow ($\Delta t = r/\nu$).

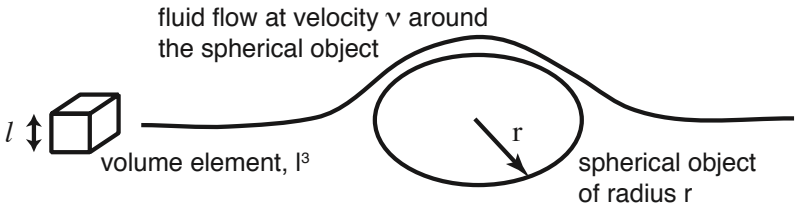

- The rate of change in velocity, dv/dt, will be approximately $\nu/\Delta t$, or $\nu/(r/\nu)$, thus ν^2/r.
- The mass of the volume element is $l^3 \bullet \rho$, where ρ is the density of the volume element.

recalling that $F = m \bullet a = m \bullet (d\nu/dt)$, we can substitute the mass and dν/dt relations described above to obtain the inertial forces:

$$F_{inertial} = (l^3 \bullet \rho) \bullet \left(\upsilon^2 / r \right)$$

units : $\dfrac{\text{cm}^3 \bullet \text{ gm cm}^{-3} \bullet \text{ cm}^2 \text{ sec}^{-2}}{\text{cm}}$

gm cm sec^{-2}

Now, we need to consider the frictional force due to the viscosity of the fluid.

[1]Source: Nelson P (2004) Biological Physics. WH Freeman and Co. pp. 163–169.

$$R_e \approx \frac{\upsilon \bullet L \bullet \rho}{\eta}$$

To explore the frictional force, it is easiest to simplify. Consider two plates moving in relation to the each other, separated by a fluid layer of thickness, d[1].

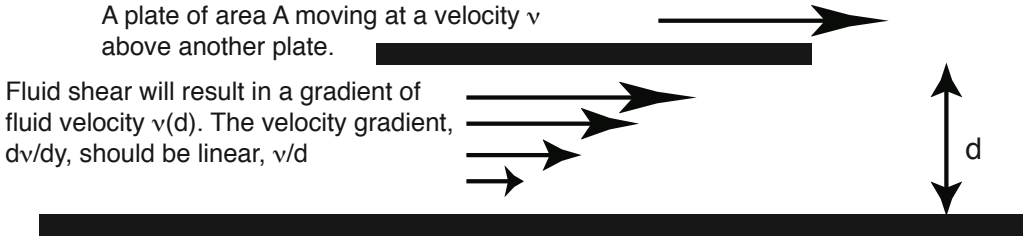

- The frictional force will depend upon the velocity at which the plate is moving (ν)
- It will be proportional to the area of the plate (A).
- The fluid shear will be proportional to the fluid viscosity (η)

Viscosity will increase the frictional force as will velocity and the plate area

$$F_{frictional} = -\left(\eta \bullet \upsilon \bullet A / d\right)$$

$$\text{units}: \frac{\text{gm cm}^{-1}\ \text{sec}^{-1} \bullet\ \text{cm sec}^{-1} \bullet \text{cm}^2}{\text{cm}}$$

$$\text{gm cm sec}^{-2}$$

But the frictional force will decrease if the distance between the two plates is increased.

This relation must be modified for fluid flow around a sphere, For the volume element moving around the spherical object, the velocity is not a uniform gradient. Thus the term ν/d in the $F_{frictional}$ equation must be replaced by dν/dx:

The area, A, is the surface area of the volume element, l^2.

$$F_{frictional} = -\eta \bullet A \bullet \left(d\nu / dx\right) \qquad F_{frictional} = -\eta \bullet l^2 \bullet \left(d\nu / dx\right)$$

[1]Source: Nelson P (2004) Biological Physics. WH Freeman and Co. pp. 163–169.

$R_e \approx \frac{\upsilon \bullet L \bullet \rho}{\eta}$

The net frictional force on the volume element is the force exerted by the volume element above, minus the force the volume element exerts on the volume element below.

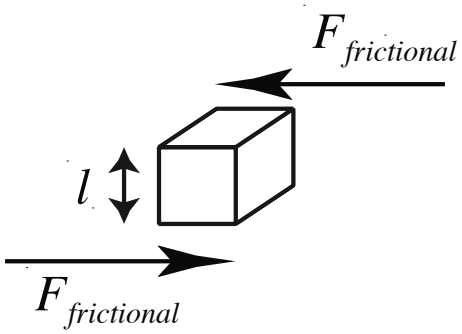

That is, net $F_{frictional} = l \bullet \left(dF_{frictional} / dx \right)$

since $F_{frictional} = -\eta \bullet l^2 \bullet \left(d\nu / dx \right)$

$dF_{frictional} / dx = -\eta \bullet l^2 \bullet \left(d^2\nu / dx^2 \right)$

and the net $F_{frictional}$, $l \bullet \left(dF_{frictional} / dx \right)$

is $F_{frictional} = -\eta \bullet l^3 \bullet \left(d^2\nu / dx^2 \right)$

But, we need to evaluate $d^2\nu/dx^2$. Since the velocity ν must change appreciably over distance comparable to the spherical object radius r: $d^2\nu / dx^2 \approx \nu / r^2$

So: $F_{frictional} = -\eta \bullet l^3 \bullet \left(\nu / r^2 \right)$

units: $\frac{\text{gm cm}^{-1} \text{ sec}^{-1} \bullet \text{ cm}^3 \bullet \text{cm sec}^{-1}}{\text{cm}^2}$

gm cm sec^{-2}

And finally, the ratio of inertial and frictional forces:

$$\frac{F_{inertial}}{F_{frictional}} = \frac{l^3 \bullet \rho \bullet \nu^2 / r}{\eta \bullet l^3 \bullet \left(\nu / r^2 \right)} = \frac{\rho \bullet \nu \bullet r}{\eta} = R_e$$

The Reynolds Number.

[1]Source: Nelson P (2004) Biological Physics. WH Freeman and Co. pp. 163–169.

The consequences of high Reynolds number can be considered from one aspect of 'design for mobility', streamlining and the concordant experimental value, the drag coefficient.

Below are examples of drag coefficients versus Reynolds Number for various examples of geometric shapes, and a streamlined shape, for which biological examples are shown in the second graph. Streamlining is important for fish and birds, which move at relatively high speeds and therefore have a high Reynolds number. Streamlining minimizes the drag that is caused by turbulence as the fish or bird moves through the water or air, respectively[1].

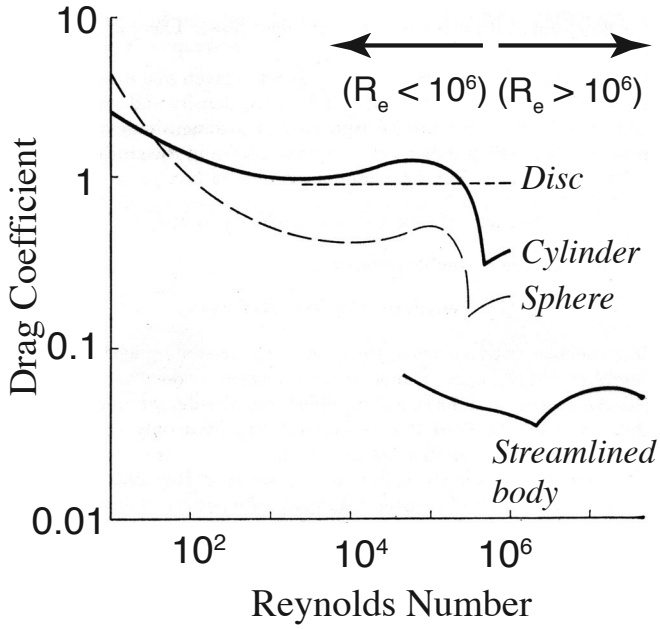

Note the discontinuity at a Reynolds number of about 10^6. This is the region where a turbulent flow boundary is formed at the front of the object. Streamlined shapes (side-views and top-views are shown below for trout, squid and a pigeon) cause lower drag both below and above the Reynolds number at which boundary turbulence occurs.

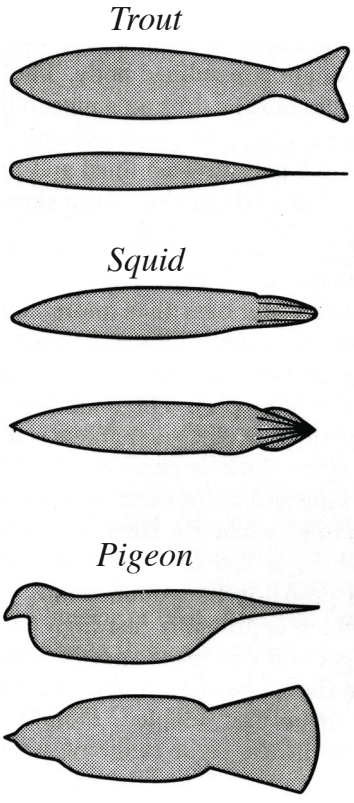

The drag (D) on an object is defined by:

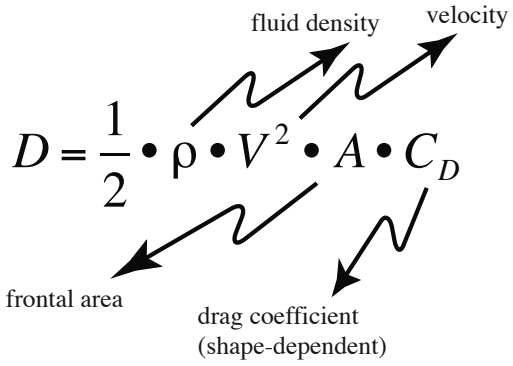

[1]Source: Alexander, R. McNeill (1971) Size and Shape. Edward Arnold Ltd. pp. 34–42.

The situation is very different when the Reynolds number is low (less than 1). Under these circumstances, viscosity dominates. For cells, such as bacteria and unicellular eukaryotes, D'Arcy Thompson described "a third world, where the bacillus lives" by stating that "we have come to the edge of a world of which we have no experience, and where all our preconceptions must be recast."[1]. For unicellular eukaryotes and bacterium, the Reynolds number can be calculated as:

$$R_e = \frac{\upsilon \bullet L \bullet \rho}{\eta} = \frac{\begin{matrix}10^{-2}\\10^{-3}\end{matrix}\ \text{cm sec}^{-1} \bullet \begin{matrix}10^{-3}\\10^{-4}\end{matrix}\ \text{cm} \bullet 1\ \text{gm cm}^{-3}}{10^{-2}\ \text{gm cm}^{-1}\text{sec}^{-1}} = \begin{matrix}10^{-3}\ \text{unicellular eukaryote}\\10^{-5}\ \text{bacterium}\end{matrix}$$

The dynamic nature of a cell at Low Reynolds Number can be illustrated by considering inertial motion: How far a bacteria would coast if it stopped swimming[2]?

For a spherical shape, and, invoking Newton's Second Law of Motion (Force = mass • acceleration), the deceleration is described by:

$$m\left(-\frac{d\upsilon}{dt}\right) = 6 \bullet \pi \bullet \eta \bullet \mathrm{r} \bullet \upsilon$$

mass of the sphere

$$\frac{4}{3} \bullet \pi \bullet \mathrm{r}^3 \bullet \rho$$

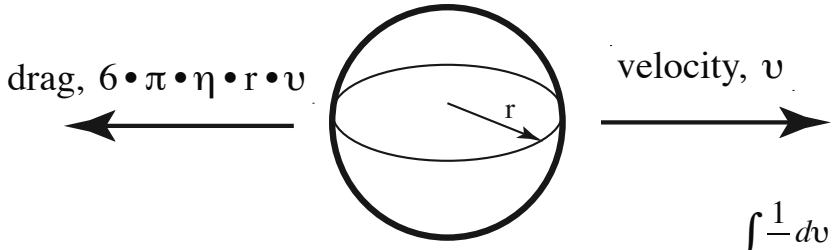

In other words, inertial momentum (m•[dv/dt]) versus the drag on the sphere.

re - arranging $m\left(-\frac{d\upsilon}{dt}\right) = 6 \bullet \pi \bullet \eta \bullet \mathrm{r} \bullet \upsilon$

$$\frac{1}{\upsilon} d\upsilon = -\frac{6 \bullet \pi \bullet \eta \bullet \mathrm{r}}{m}\ dt$$

the integration solution is:

$$\upsilon(\mathrm{t}) = \upsilon_0 e^{\left(-\frac{6\bullet\pi\bullet\eta\bullet r}{m}\bullet t\right)}$$

$$\int \frac{1}{\upsilon} d\upsilon = \int -\frac{6 \bullet \pi \bullet \eta \bullet r}{m} dt$$

$$\ln(\upsilon) = -\frac{6 \bullet \pi \bullet \eta \bullet r}{m} \bullet t + A$$

$$\upsilon(t) = e^{\left(-\frac{6\bullet\pi\bullet\eta\bullet r}{m}\bullet t\right)} \bullet e^{A}$$

At time $t = 0$, $e^{\left(-\frac{6\bullet\pi\bullet\eta\bullet r}{m}\bullet t\right)} = 1$

so, $e^{A} = \upsilon_0$, thus

$$\upsilon(\mathrm{t}) = \upsilon_0 e^{\left(-\frac{6\bullet\pi\bullet\eta\bullet r}{m}\bullet t\right)}$$

[1]Source: Thompson, D'Arcy (1961) On Growth and Form. Cambridge University Press. pp.48.

[2]Source: Berg, Howard C. (1993) Random Walks in Biology. Princeton University Press. pp. 76–77.

The time required for a bacterium (10^{-4} cm sphere) to decelerate from an initial velocity of 20 μm sec^{-1} is shown below[1]:

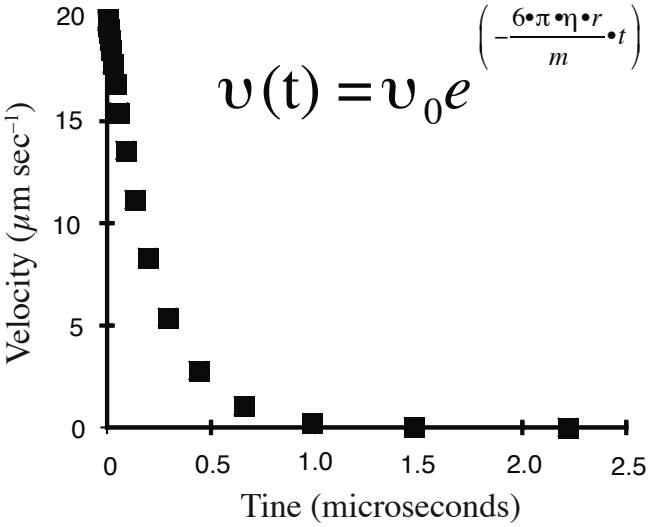

$$\upsilon(t) = \upsilon_0 e^{\left(-\frac{6 \bullet \pi \bullet \eta \bullet r}{m} \bullet t\right)}$$

$\eta = 10^{-2}$ gm cm^{-1} sec

$r = 10^{-4}$ cm

$$m = \frac{4}{3} \bullet \pi \bullet 1 \text{ (gm cm}^{-3}) \bullet (10^{-4} \text{ cm})^3$$

Deceleration is very fast, occurring within 3.0 microseconds.

The distance it would travel can be approximated: 20 μm sec^{-1} times τ ($\tau = 6\pi\eta r/m$)(0.22 microseconds): about $4.44 \bullet 10^{-10}$ cm, less than the width of an atom.

By comparison, a fish swimming at 20 cm sec^{-1}would coast to a stop in about 180 seconds, traveling a distance of about 11 meters. So, D'Arcy Thompson's description is very reasonable: Bacteria live in a very different world than ours, where viscosity dominates rather than inertia.

How then does a bacteria swim? This will be addressed in the next section.

[1]Source: Berg, Howard C. (1993) Random Walks in Biology. Princeton University Press. pp. 76–77.
Purcell E.M. (1977) Life at low Reynolds number. American Journal of Physics 45:3–11.

So how does a bacterium move? First, they do swim, at rates of about 20 μm sec^{-1}. But before considering the mechanism of motility, it is worthwhile to examine the swimming behaviour of bacteria. A diagram of bacterial swimming is shown below. The location of the bacteria has been mapped at 0.079 second intervals (12.6 dots sec^{-1})[1]:

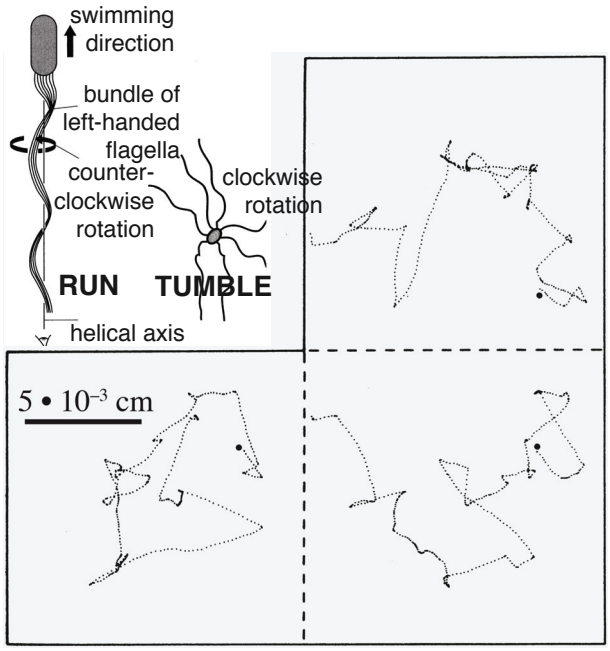

A digital plot of a wildtype bacterium (E. coli) swimming in a homogeneous isotropic medium. The plots are planar projections of a three dimensional path (folding the left and upper panels along the dashed lines would re-create the three dimensional plot). The large dot indicates the beginning of the plot. Runs (flagella turning counter-clockwise, resulting in directional swimming) can be identified by the increased spacing between dots. Tumbles (flagella rotating clock-wise and unwinding) are relatively short in duration and end in a run that is often in a different direction from the pre-tumble run.

The shape of the swimming path is quite similar to a random walk[2]: Compare a three-dimensional random walk (right) to the bacterial path above. The trace started at the 0,0 coordinate, then moved randomly a specified distance at each time interval.

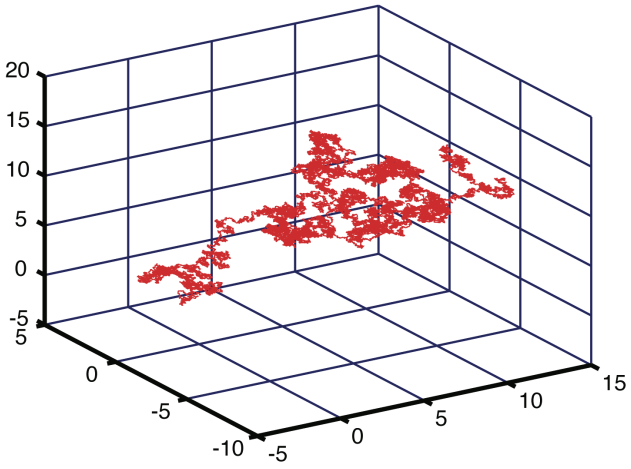

Displacements from zero (relative distance)

[1]Source: Berg, Howard C. (1993) Random Walks in Biology. Princeton University Press. pp. 80.

[2]Source: A MATLAB simulation.

The Run and Tumble swimming behaviour of bacteria is quite common. Although the tumbling events are random, the timing of the Run and Tumble intervals will vary if a bacteria is placed in a gradient of some chemical (for example, amino acids or glucose) that are used as either building blocks (amino acids for protein synthesis) or energy (glucose)[1].

Receptor	Attractant	Repellant	
Tsr	serine, cysteine, alanine	indole, H^+	The receptors can be identified by screening for bacteria mutants which do not exhibit chemoattraction to a specific chemical. The screen would involve scoring for presence or absence of congregation near the chemical source.
Tar	aspartate, maltose, glutamate, H^+	Ni^{2+}, Co^{2+}	
Tap	dipeptides	H^+	
Trg	galactose, ribose, H^+		Glucose-sensing involves the normal uptake pathway, rather than a specialized receptor. Note the oxy-sensing, important for an aerobic bacterium that uses oxidative phosphorylation to produce ATP.
Aer	O_2		

Below is shown an example of the Run and Tumble (vertical bars) behaviour of the bacterium in response to the addition of a chemo-attractant. Note the decrease in tumbling when attractant is present (because the bacterium no longer needs to 'search' for nutrients. When attractant is removed, tumbling rates increase dramatically, as the bacterium searches the three-dimensional space for higher concentrations of nutrients. The Run and Tumble behaviour of the bacterium is still random, in the sense that the timing of the tumbles is random, but the frequency increases. Probabilities for such discrete random events are described by the Poisson Distribution.

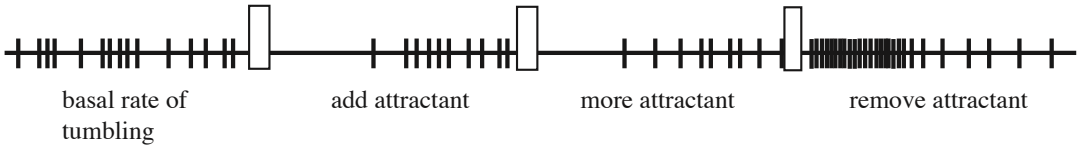

[1]Source: Bray, Dennis (2001) Cell Movements. From molecule to motility. Chapter 16 (Bacterial Movements). Garland Publishing pp. 257–274.

The bacterial cell switches back and forth between Run and Tumble modes at random (this behaviour requires that the motor switch from counter-clockwise rotation to clockwise rotation). The probability that a tumble event will occur is assumed to be a constant (average) probability (λ) for a specified unit time (λdt). This average probability varies in the presence or absence of chemo-attractant.

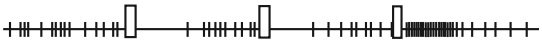

The behaviour of the Run and Tumble is described by Poisson statistics. The Poisson distribution is relevant to many physical approaches to biological problems. It is not as widely used as the Gaussian (normal) distribution, so it tends to be presented as an afterthought in error analysis and statistics courses. Nevertheless, it is useful in analyses for which event probabilities are small, like the tumble events of a bacterial Run and Tumble. So, here is an explanation of its roots and uses.

The key equation that describes the Poisson distribution is: $$\frac{e^{-\mu}\mu^{k}}{k!}$$

This is the probability $p(k,\mu)$ that k number of events will occur. The mean number of events is μ, and the standard devation is $\mu^{1/2}$.

The distribution was described by Poisson in 1837, but a far more thorough description of the statistics of rare events was presented by von Bortkiewicz, who wrote a thesis entitled "The Law of Small Numbers" in 1898. In his thesis, von Bortkiewicz presented a famous data set that is an excellent example of the kind of data that can be described by the Poisson distribution: Death by Horse-Kick in Prussian Army Corps. The data are a compilation of horse-kick deaths over a period of 20 years in fifteen army corps[1]:

Table 1. Bortkewitsch's data table, giving numbers of deaths from horse-kicks

	Year																			
Corps	1875	1876	1877	1878	1879	1880	1881	1882	1883	1884	1885	1886	1887	1888	1889	1890	1891	1892	1893	1894	Totals
G	0	2	2	1	0	0	1	1	0	3	0	2	1	0	0	1	0	1	0	1	16
I	0	0	0	2	0	3	0	2	0	0	0	1	1	1	0	2	0	3	1	0	16
II	0	0	0	2	0	2	0	0	1	1	0	0	2	1	1	0	0	2	0	0	12
III	0	0	0	1	1	1	2	0	2	0	0	0	1	0	1	2	1	0	0	0	12
IV	0	1	0	1	1	1	1	0	0	0	0	1	0	0	0	0	1	1	0	0	8
V	0	0	0	0	2	1	0	0	1	0	0	1	0	1	1	1	1	1	1	0	11
VI	0	0	1	0	2	0	0	1	2	0	1	1	3	1	1	1	0	3	0	0	17
VII	1	0	1	0	0	0	1	0	1	1	0	0	2	0	0	2	1	0	2	0	12
VIII	1	0	0	0	1	0	0	1	0	0	0	0	1	0	0	0	1	1	0	1	7
IX	0	0	0	0	0	2	1	1	1	0	2	1	1	0	1	2	0	1	0	0	13
X	0	0	1	1	0	1	0	2	0	2	0	0	0	0	2	1	3	0	1	1	15
XI	0	0	0	0	2	4	0	1	3	0	1	1	1	1	2	1	3	1	3	1	25
XIV	1	1	2	1	1	3	0	4	0	1	0	3	2	1	0	2	1	1	0	0	24
XV	0	1	0	0	0	0	0	1	0	1	1	0	0	0	2	2	0	0	0	0	8
Total	3	5	7	9	10	18	6	14	11	9	5	11	15	6	11	17	12	15	8	4	196

[1]Preece, DA, GJS Ross, PJ Kirby (1988) Bortkewitsch's horse-kicks and the generalized linear model. Journal of the Royal Statistical Society Series D (The Statistician). 37(3):313–318.

If we select data from von Bortkiewicz for a single army corps and graph the number of horse-kick deaths *versus* year:

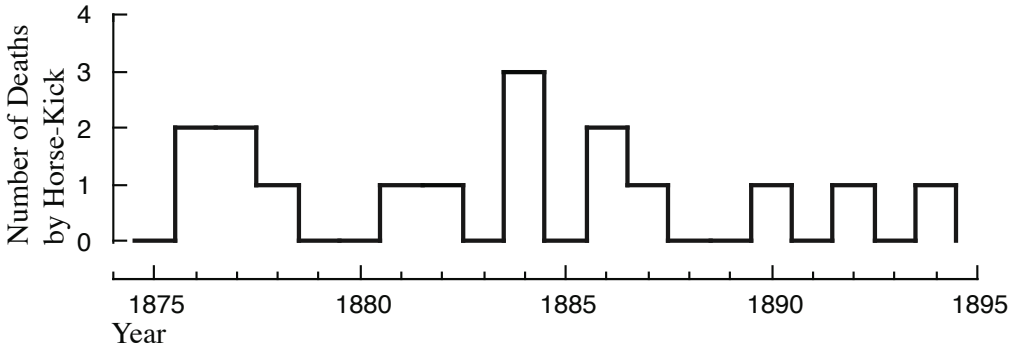

The 'spikey' nature of the events are similar to the run and tumbling events of the bacteria:

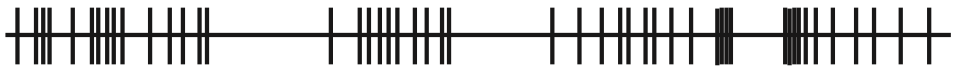

And similar to the opening/closing events of an ion channel in a biological membrane:

In all three examples, the events are relatively rare, appear to occur randomly, and are independent of each other.

How can we describe such random, rare events? We need to rely upon a description of the probability of the events. The average probability that an event will occur per unit time (that is, an average frequency of events),

$$\lambda = \frac{\text{average number of events}}{\text{unit of time}}$$

when multiplied by the time interval, will tell us the probability that an event will occur:

$$p(t) = \lambda \bullet t$$

An analysis of the probability of a rare and random event occurring in a time interval, t, is eased by considering the converse case, the probability that No Event will occur in the time interval, t. This is equivalent to the probability that no horse-kick deaths occur, a channel does not open, or the bacteria remains in a Run mode during the time interval t.

In this case, the probability of an event

$$p(t) = \lambda \bullet t$$

is re-cast as the probability that no event will occur:

$$p_o(t) = 1 - \lambda \bullet t$$

By expressing the probability equation in the form of an infinitesimal time, δt, we can use limit analysis. First the probability of no event during the interval t + δt, is the product of the probability in the time interval, t, and the probability in the time interval δt.

$$p_o(t + \delta t) = p_o(t)(1 - \lambda \bullet \delta t)$$

At the limit, δt approaches zero:

$$\lim_{\delta t \to 0} \; p_o(t + \delta t) = p_o(t)(1 - \lambda \bullet \delta t)$$

The resulting differential equation is:

$$\frac{\partial p_o}{\partial t} = -\lambda p_o(t)$$

For which the solution is: $p_o(t) = e^{-\lambda t}$

$$p_o(t + \delta t) = p_o(t)(1 - \lambda \bullet \delta t) = p_o(t) - \lambda p_o(t)\delta t$$

dividing by δt and subtracting the term $p_o(t)$

$$\frac{p_o(t + \delta t)}{\delta t} - \frac{p_o(t)}{\delta t} = \frac{p_o(t + \delta t) - p_o(t)}{\delta t} = -\lambda p_o(t)$$

$$\lim_{\delta t \to 0} \frac{p_o(t + \delta t) - p_o(t)}{\delta t} = \frac{\partial p_o}{\partial t} = -\lambda p_o(t)$$

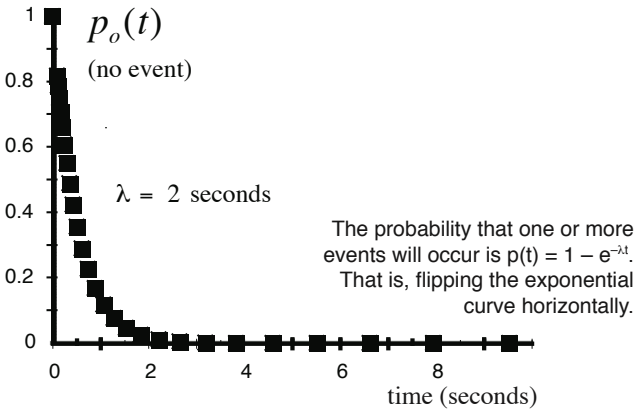

Re - arranging and integrating over the time interval t = 0 to t = t

$$\int_{t=0}^{t=t} \frac{1}{p_o(t)} dp_o = \int_{t=0}^{t=t} -\lambda dt$$

$$\Big|_{t=0}^{t=t} \ln p_o(t) = \Big|_{t=0}^{t=t} -\lambda t$$

since $p_o(0)$ must be unity ($\ln(1) = 0$) and $\lambda \bullet 0 = 0$, then

$-\ln(p_o(t)) = \lambda t$, or $\ln(p_o(t)) = -\lambda t$, and

$p_o(t) = e^{-\lambda t}$

To arrive at the Poisson distribution itself is challenging. Essentially, we are no longer interested in a probabillity for a single event, but instead, the probability for multiple events. The easiest way to begin is to consider one event, p_1[1]. We need to integrate over the time duration T, in which an event occurs at time t + δt, but not at time 0 to t or time t to T

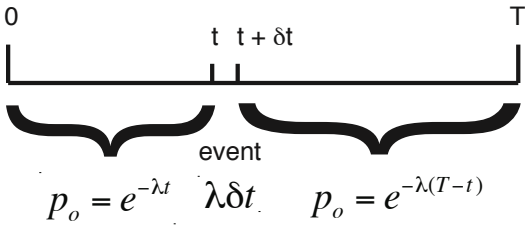

$$p_1 = \int_0^T e^{-\lambda t} e^{-\lambda(T-t)} \lambda dt = e^{-\lambda T} \lambda T$$

If there are two events: λδ*t* and λ(T-*t*), then

$$p_2 = \int_0^T e^{-\lambda t} e^{-\lambda(T-t)} \lambda(T-t) \lambda dt = e^{-\lambda T} \frac{(\lambda T)^2}{2}$$

If there are n events:

$$p_n = e^{-\lambda T} \frac{(\lambda T)^n}{n!}$$

This equation is the same as:

$$\frac{e^{-\mu} \mu^k}{k!}$$

where μ = λT and k = n.

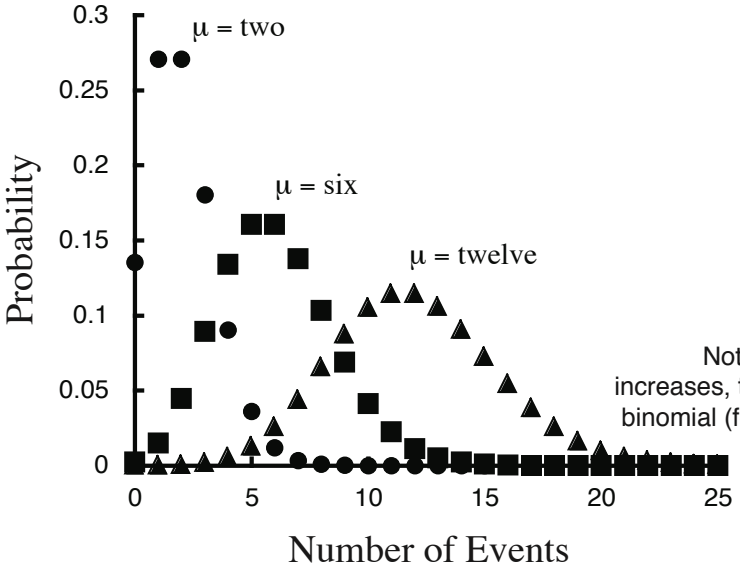

Note that as the number of events increases, the distribution approaches the binomial (for discrete events) distribution.

[1]MacDonald, DKC (1962) Noise and Fluctuations. (reprinted 2006, Dover Publications). Appendix IV. pp. 109–110.

The examples so far have been in the form of events that occur over time. Other examples of such time dependent processes that are important to Biophysics include radioactive decay and particle bombardment. Bombardment has many applications (besides high energy particle accelerators); clinical applications include tumour bombardment in cancer treatments. Another example is the determination of target size of proteins[1], to determine molecular weight. In both, successful hits are described by Poisson statistics.

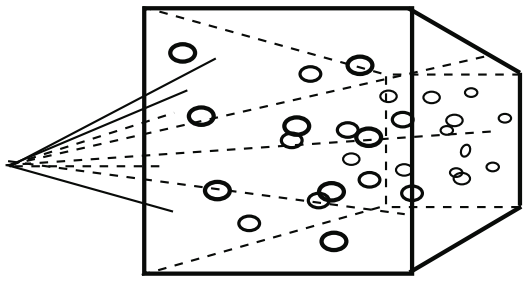

As the radiation passes through the system, there is some probability that ionizations (1, 2, 3 ... ionizations) will occur in some unit volume. That probability is the Poisson distribution. It is assumed that an ionization event will render the protein or cell inactive (or dead).

The Poisson distribution for n number of ionizations depends upon some measure of the amount of radiation exposure, x.

$$p_n = \frac{e^{-x} x^n}{n!}$$

In radiation inactivation to determine the molecular weight of a protein, we are interested in the survivors, that is p_0:

$$p_0 = \frac{e^{-x} x^0}{0!} = e^{-x}$$

$$A = A_0 e^{-kD}$$

We can transform the equation to assess the activity remaining, A (relative to the initial activity A_0), the target size (k, dependent on the density of proteins and Avogadro's Number), and the radiation dosage, D (in units of primary ionizations per unit volume)

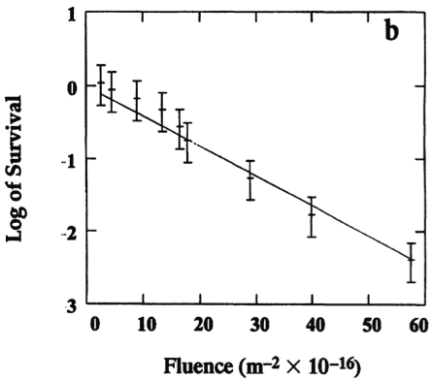

Here is an example of a survival versus radiation dose curve for an enzyme (peroxidase in this example), where the y-axis is log(survival), transforming to a linear relation. From the slope, the predicted molecular weight of the enzyme is 24 kDa.

Now, back to the run and tumble world of bacteria...

[1]Kempner ES, W Schlegel (1979) Size determination of enzymes by radiation inactivation. Analytical Biochemistry 92:2–10.

In the case of bacterial motility, the utility of the Poisson distribution is to explore the randomness of Runs and Tumbles, but it is also used to explore the nature of motility.

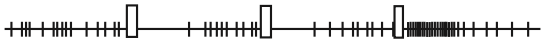

Here is an example for an extremophile: *Sulfolobus acidocaldarius*. As the name may suggest, this bacteria grows optimally at 75 to 80°C and pH 2 to 3 in terrestrial solfataric springs. 'Solfatara' is defined as "A volcanic area that gives off sulfurous gases and steam".

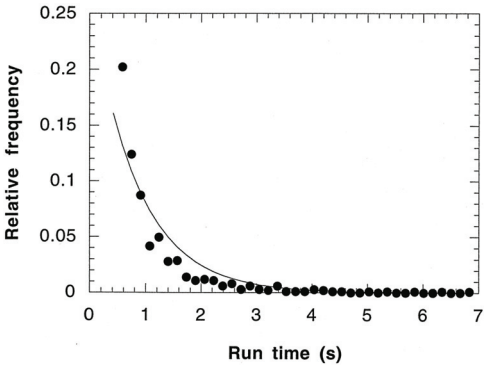

The distribution of run times (circles) is plotted with a best-fit to a Poisson distribution (solid line) to demonstrate that the duration of runs is close to random. The experiments were performed at 60°C and pH 3. The mean run time was 0.62 ± 0.92 s.

Lewus P and RM Ford (1999) Temperature-sensitive motility of Sulfolobolus acidocaldarius influences population distribution in extreme environments. Journal of Bacteriology 181:4020–4025.

Both swimming speed and average run times increase with increasing temperature. Why would this occur? Given where this bacterium lives, it may be an adaptive strategy, to escape quickly (if 10–15 μm/sec can be considered fast) from temperatures that are too high.

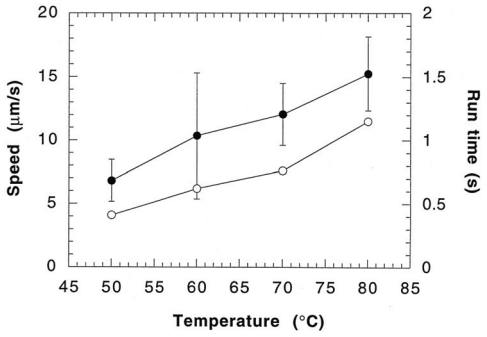

Lewus P and RM Ford (1999) Temperature-sensitive motility of Sulfolobolus acidocaldarius influences population distribution in extreme environments. Journal of Bacteriology 181:4020–4025.

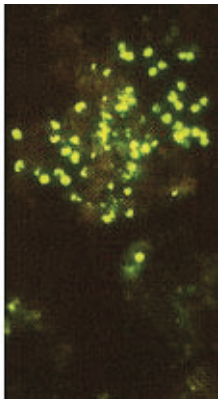

Electron micrograph of Sulfolobolus acidocaldarius (left) and fluorescent micrograph (right) showing cells attached to sulfur crystals.

When the bacterium Tumbles, it usually commences its next run in a different direction. The turn angle is also a bacteria-specific property.

Turn angles for *Sulfolobus acidocaldarius* are shown, as well as data for *Escherichia coli* and *Pseudomonas putida*. *Escherichia coli* is a normal member of the human intestinal flora. *Pseudomonas putida* resides in soil.

Sulfolobolus acidocaldarius exhibits less of a turn angle that Escherichia coli, probably because Sulfobolus flagella do not reverse, decreasing the extent of tumbling. Both bacteria have unimodal distributions of turn angles. The soil-dwelling bacterium Pseudomonas putida exhibits a bimodal distribution of turn angles, probably adaptive for avoiding collisions in its obstacle-crowded environment.

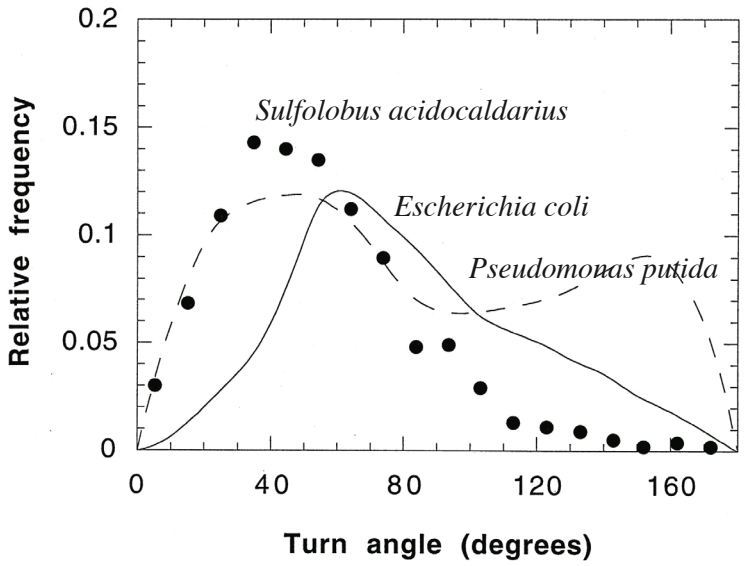

Lewus P and RM Ford (1999) Temperature-sensitive motility of Sulfolobolus acidocaldarius influences population distribution in extreme environments. Journal of Bacteriology 181:4020–4025.

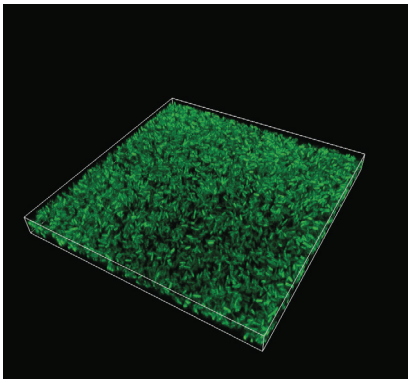

Three dimensional reconstruction of a biofilm as imaged with two-photon microscopy; pure culture biofilm of a GFP-mutant Pseudomonas putida.

JAMES D. BRYERS
THE CENTER FOR BIOMATERIALS
http://www.uchc.edu/biomaterials/Res.Int.James.html

Historically, two approaches have been used to determine the structure and mechanism of the flagellar motor: Molecular Genetics and Structure Imaging (usually with electron microscopy). There are a number of major functional components (the total protein ensemble is about 33 unique units): A cylindrical rod extends from a C-ring complex and passes through a hollow ring of proteins at the periplasmic membrane (a 'bushing'), ending in a hook, from which the flagellum extends, made up of flagellin subunits. The flagellin subunits form a hollow cylinder (ID 3 nm, OD 20 nm). Notably, assembly of the flagella involves diffusion of the flagellin subunits through the hollow core to the flagellum tip, where *de novo* assembly occurs. The complex at the cytoplasmic membrane is often described as a stator/rotor assembly, analogous to the stator/rotor of an electric motor.

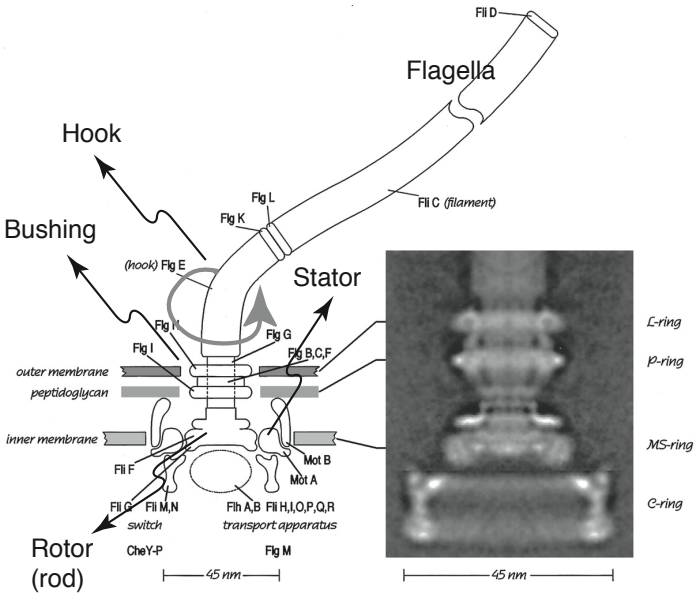

A schematic diagram of the flagellar motor, drawn to scale, compared to a rotationally averaged reconstruction of images of hook-basal bodies seen in an electron microscope. The general morphological features are C-ring, MS-ring, P-ring, L-ring, hook, hook-associated proteins (which include the distal cap), and filament. MotA, MotB, and components of the transport apparatus (dashed ellipse) do not survive extraction with detergent and, therefore, are not shown on the right. The radial densities have been projected from front to back along the line of view, so this is what would be seen if one were able to look through the spinning structure. Connections between the C-ring and the rest of the structure appear relatively tenuous. From: Berg, HC (2003) The rotatory motor of bacterial flagella. Annual Review of Biochemistry 72:19–54.

Direct evidence for the rotatory motion of the flagella comes from experiments in which the hook is adhered to a glass slide, so that the rotation of the bacterial body can be observed. Rotational speeds under normal conditions are estimated to range from 18,000 rpm (300 Hz) to 100,000 rpm (1700 Hz)[1]. But how? Where does the energy come from?

[1]Source: Bray, Dennis (2001) Cell Movements. From molecule to motility. Chapter 16 (Bacterial Movements). Garland Publishing pp. 257–274.

The heart of the rotatory NanoMotor is its energy source. The reaction can be described by a chemical equation:

$$\text{Rotor}_{(n)} + m H^{+}_{\text{outside}} \longleftrightarrow \text{Rotor}_{(n+1)} + m H^{+}_{\text{inside}}$$

In which the transport of H^+ (or Na^+) from the periplasmic space to the inside of the cytoplasmic membrane is coupled to incremental rotation of the rotor (from n to n+1).

A similar reaction occurs in the synthesis of ATP by the ATP synthetase (also found in the cytoplasmic membrane of bacteria as well as the inner membranes of mitochondria and chloroplasts):

$$ADP + P_i + mH^{+}_{\text{outside}} \longleftrightarrow ATP + mH^{+}_{\text{inside}}$$

For the latter case, the energetics are described by the chemical potential for the H^+ ($\Delta\mu$) and the Gibbs free energy (ΔG) for the chemical reaction of ATP synthesis:

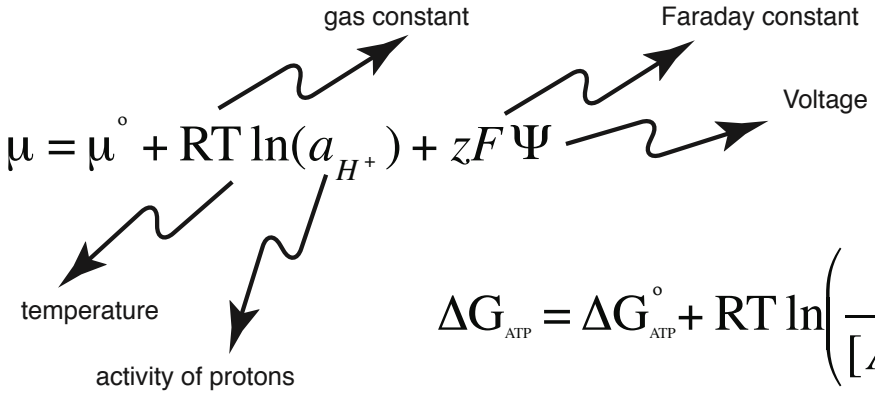

These are biological descriptions of energetics. The chemical potential can be equated with the Gibbs free energy to determine stoichiometry of the chemical reaction (three protons are required to synthesize one ATP molecule).

The structure of the ATP synthase has similarities to the flagellar motor, especially evidence that rotation of the c complex in the membrane cause conformational change that are transduced into ATP synthesis from ADP and phosphate.

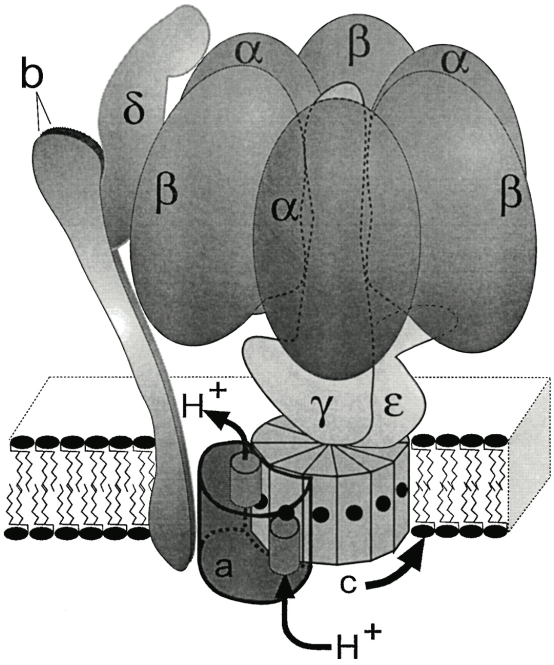

Schematic subunit arrangement of the Escherichia coli F_0F_1 ATP synthase and the proposed proton pathway in F_0. The $\alpha_3\beta_3$ hexamer containing the catalytic sites in each of the β subunits surrounds the rotor shaft made up of the γ subunit coiled-coil. The rest of the proposed rotor consists of the ε and c subunits. The stator $\alpha_3\beta_3$ and a subunits are connected by the δ and two b subunits. The 10–12 c subunits are believed to be arranged in a ring, with subunit a on the side. Proton transport is mediated between the a and c subunits. As shown, the protons enter from the periplasmic space (right half-channel) to protonate the c subunit, and the protonated c subunit rotates counterclockwise until it meets the cytoplasmic-facing half-channel (left), where the protons are released. Nakamoto RK, CJ Ketchum and MK Al-Shawi (1999) Rotation coupling in the F_0F_1 ATP synthase. Annual Review of Biophysics and Biomolecular Structure. 28:205–234.

$$ADP + P_i + mH^+_{outside} \longleftrightarrow ATP + mH^+_{inside}$$

Energetic equivalence of the chemical potential and Gibbs free energy at equilibrium:

$$\Delta G_{total} = n \bullet \Delta\mu_{H^+} + \Delta G_{ATP} = 0$$

$$n \bullet \left(RT \ln\left(\frac{a^{inside}_{H^+}}{a^{outside}_{H^+}}\right) + F\Delta\Psi\right) + \Delta G^o_{ATP} + RT \ln\left(\frac{[ATP]}{[ADP][P_i]}\right) = 0$$

The equilibrium energy is determined by solving for $\Delta\Psi$

(ΔG^o_{ATP} and H^+ activities can be determined experimentally, as can [ATP], [ADP] and $[P_i]$).

Biochemists identified the role of the proton motive force in ATP synthesis and bacterial motility over a period of time extending from the 1950's through the 1990's. Much of this scientific history is embedded in introductory and advanced biochemistry textbooks in various forms.

It is, however, highly unlikely that the proton (H^+, a positively charged hydrogen ion) could be the transported ion. It is very small, with a correspondingly high charge density, difficult to polarize, and unlikely to exist for more than a brief moment in aqueous biological environs, where there are so many other molecules it can interact with (especially water molecules, H_2O, but also ionizable groups such as carboxyls, aminos and phosphates). If it did react with H_20, the product would be the hydronium ion H_3O^+.

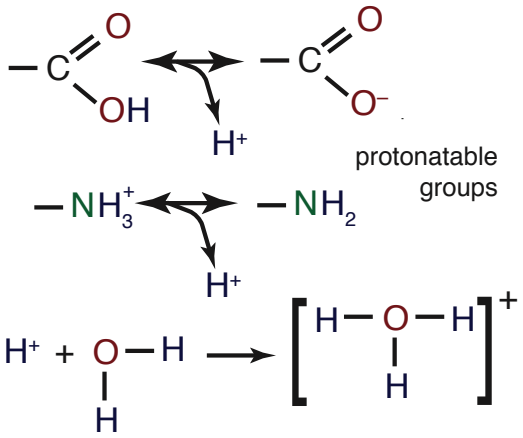

This is important in the context of flagellar rotation (or ATP synthesis), because the mechanisms using a naked proton H^+ would be different from those involving H_3O^+. The hydrogen ion would tend to pass from one ionizable group to the next (often called a proton wire). This could result in conformational changes that cause a torsional strain and eventually rotation. The H_3O^+ would have to pass through a pore structure[1]. Now, the actual mechanism could involve a combination of both proton wire and hydronium ion pore, but in fact this is not the case. The reason for such certainty is that certain bacteria rely upon Na^+ motive force, rather than H^+ motive force for synthesis of ATP and flagellar rotation[2]. Unlike the naked proton H^+, the Na^+ ion will not react with ionizable groups by forming a covalent bond.

Hydronium ion depictions

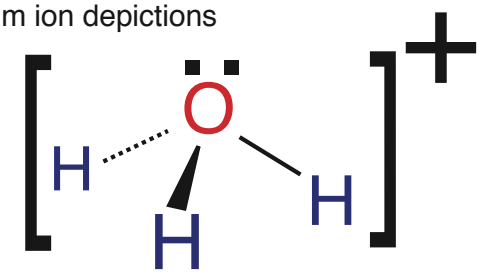

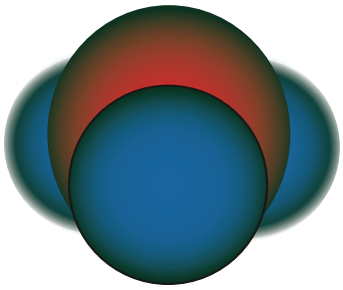

[1]Source: Boyer, PD (1988) Bioenergetic coupling to proton motive force: Should we be considering hydronium ion coordination and not group protonation? Trends in Biochemical Science 13:5–7.

[2]Source: Dimroth P (1995) On the way towards the Na^+-binding site within the F_1F_o ATPase of *Propionigenium modestum*. Biochem. Soc. Trans. 23:770–775.

In the case of rotatory motion, the difficulty is how to determine the free energy of rotation. This is problematic for a number of reasons. Recall that the rotatory reaction can be described by a chemical equation:

$$\text{Rotor}_{(n)} + m H^+_{\text{outside}} \longleftrightarrow \text{Rotor}_{(n+1)} + m H^+_{\text{inside}}$$

First, we need to know the stoichiometry. That is, the number of H^+ passing through the motor per complete rotation of the rotor.

Second, we need to know the efficiency of coupling. That is, whether there is slippage caused by H^+ translocation without rotation, or backwards rotation.

Finally, we need to know the energy required to rotate the flagella through the solution, both the rotational and translation motion as the bacteria swims through the solution.

Present estimates of H^+ stoichiometry are about 1200 H^+ per complete revolution. Efficiencies are reported to vary from 5% at low load to 50–100% at high load[1].

In the case of the rotatory motor, it is solely the chemical potential for protons (often called the proton motive force) that is of interest. This can be manipulated experimentally, by modfiying the $[H^+]$ inside and outside, and the potential:

$$\Delta\mu_{H^+} = \frac{RT}{F} \ln\left(\frac{a^{inside}_{H^+}}{a^{outside}_{H^+}}\right) + \Delta\Psi \quad \text{(units: mV)}$$

RT/F is about 25 mV at 20ºC.

Then, the effect on rotational frequency under various loads (created by modifying the viscosity of the solution) can be examined.

[1]Source: Bray, Dennis (2001) Cell Movements. From molecule to motility. Chapter 16 (Bacterial Movements). Garland Publishing pp. 257–274.

Rotational frequency under various loads (created by modifying the viscosity of the solution) can be examined by a variety of techniques (including optical tweezers). Shown below is a direct method.

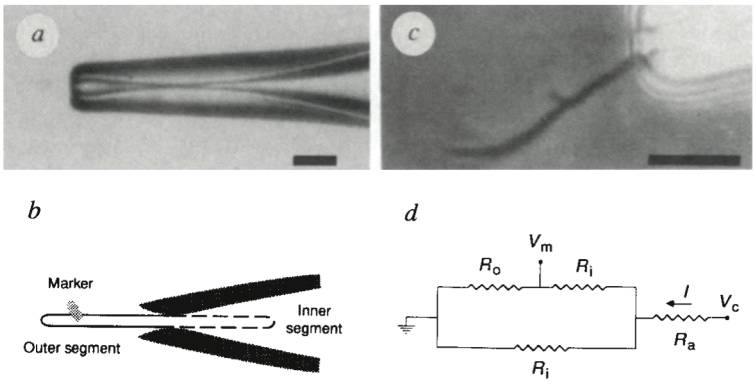

The bacterium is held in a micropipette, and a voltage applied between the inside and outside of the micropipette. Rotation is measured by recording the movement of a marker tethered to a motor. Fung DC and HC Berg (1995) Powering the flagellar motor of Escerichia coli with an external voltage source. Nature 375:809–812.

Summaries from multiple published sources are presented below: The linear dependence of the rotational frequency and the non-linear relation between torque and frequency are clear.

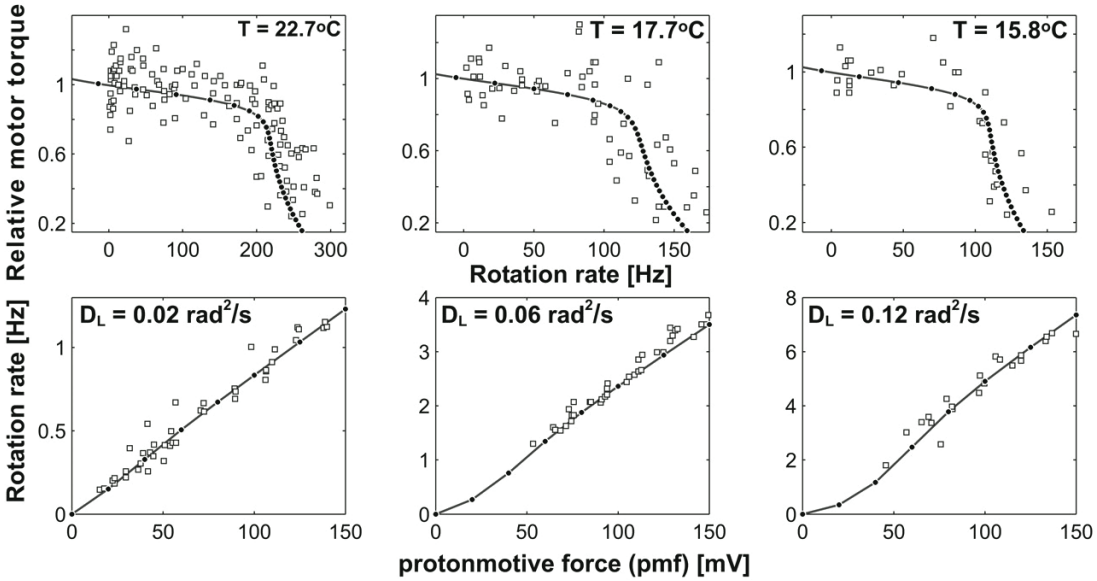

The upper graphs show torque (torque has units of N•m) versus speed at different temperatures. The lower graphs show speed versus protonmotive force at various loads (D_L). Note that the motor rotates faster at higher drag coefficients (D_L) created by increasing the medium viscosity. Experimental data are shown with open circles. One example of a predictive model is shown by filled circles. Xing J, F Bai, R Berry and G Oster (2006) Torque-speed relationship of the bacterial flagellar motor. Proceedings of the National Academy of Science USA 103:1260–1265.

The nanomotor data are worthy of close examination. The lower data demonstrate a clear linear dependence of flagellar rotation versus proton motive force. Thus, coupling between the vectorial movement of hydronium ions and a mechanical movement (rotation) is likely. What is counterintuitive is that rate of rotation is faster when the flagellar rotation is subjected to a higher load (by modifying the viscosity and thus the torque load for rotation). This latter experimental observation can be explained by invoking an elastic mechanical linkage between vectorial hydronium ion translocation and mechanical rotation. In other words, under low load, the linkage is prone to slippage, but at higher load, the elastic linkage becomes stiffer, and coupling efficiency is increased.

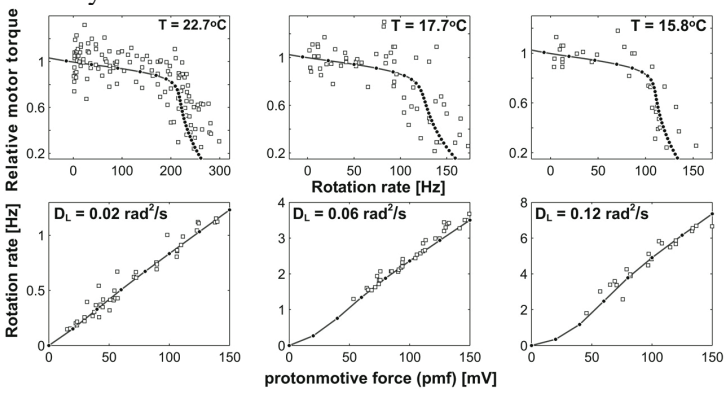

In the recent paper by Xing et al. (2006)[1], the authors propose a set of assumptions to explain the function of the flagellar motor:

Assumption A: "The rotation of the motor is observed through a soft elastic linkage between the motor and the viscous load." They identify the elasticity of the 'hook region' as the source, and note that it allows the motor and flagella to move at different characteristic time scales.

Assumption B: "Motor rotation and ion transport are tightly coupled." As a consequence, there is a linear dependence between rotation frequency and the proton (or ion) motive force.

Assumption C: "The power stroke is driven by a conformational transition in the stator that is triggered by the protons [ions] hopping onto and off the stator, probably via the MotB residue D32." The implication is that the conformational change is the rate-limiting step, not ion translocation, which is known to involve an aspartate (D32, an acidic amino acid with a ionizable carboxyl group) in the MotB subunit commonly believed to function as part of the stator of the motor.

Assumption D: "The ion channel through the stator is gated by the motion of the rotor." Thus, ion translocation through the stator will depend upon the motor speed. This is required to explain the concave shape of the torque versus speed relations, and the sharp transition from plateau (flat) to declining torque.

[1]Source: Xing J, F Bai, R Berry and G Oster (2006) Torque-speed relationnship of the bacterial flagellar motor. Proceedings of the National Academy of Science USA 103:1260–1265.

Now, Xing et al. (2006) go on to propose a model based upon changes in the potential energies associated with the step-wise coupling of ion translocation and flagellar rotation. But they freely admit that many models could be proposed that would fit the data on flagellar rotation versus ion motive force.

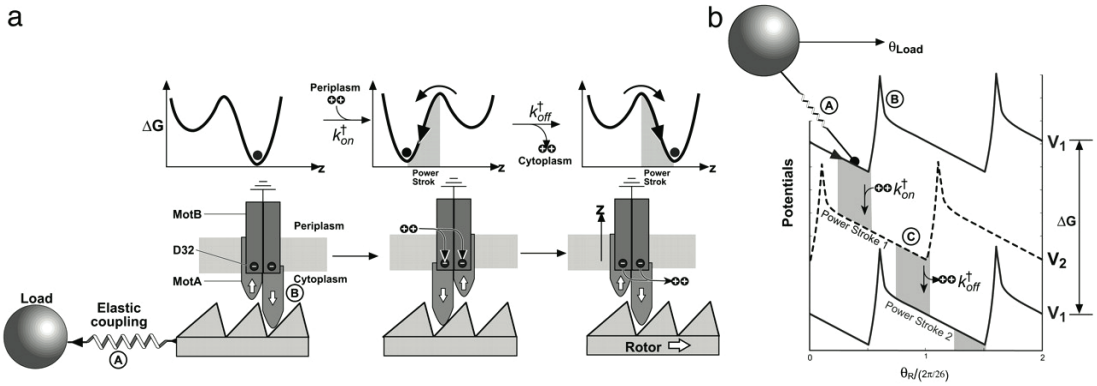

(a) Schematic illustration of one motor cycle. Step 1: at the end of previous cycle, D32 residues on the stator are unprotonated, and the stable conformation is as shown on the left; the cytoplasmic loop of one MotA (the right one in the figure) is down, engaging the rotor. Binding of two protons to the MotB D32 residues neutralizes them, allowing a thermally activated transition to the alternate conformational equilibrium to perform the first power stroke with the other MotA loop engaging the rotor. Step 2: At the end of the first power stroke, the two binding protons are released to the cytoplasm. This transition triggers another conformational change of the stator so the (right) MotA loop engages to the rotor to perform the second power stroke. At the end of the cycle, the stator has returned to its conformation at the beginning of the cycle, with the rotor advancing one step to the right. **(b)** The driving potentials (free energies) of the stator corresponding to **(a)** are approximated. The soft elastic coupling between the rotor and the load is indicated by the spring, A. Each motor cycle transports two ions from periplasm to cytoplasm, which decreases the free energy of the system by 2e x pmf and advances the rotor by 2π /26. Labels A–C correspond to Assumptions A–C in the text[1].

Real insight into the mechanism will depend on much higher resolution imaging of the protein structures, at a resolution high enough to 'see' the hydronium ion location within the pore at the various kinetic steps.

Having explored the nature of the stator-rotor structure, we now need to turn to the hows and whys of flagellar rotation and bacterial mobility.

[1]Source: Xing J, F Bai, R Berry and G Oster (2006) Torque-speed relationnship of the bacterial flagellar motor. Proceedings of the National Academy of Science USA 103:1260–1265.

The Nobel Laureate Edward M. Purcell[1] considered the mechanisms of propulsion for a bacteria. Much of his considerations are presented in a classic paper entitled "Life at low Reynolds number" (American Journal of Physics 45:3–11. 1977) (a required reading). The motility of the bacteria (with a velocity, υ) relies upon the rotation of a helical shaped flagella rotating at a frequency ω, while the bacterial body counter-rotates at a frequency Ω in the opposite direction (hence the negative value).

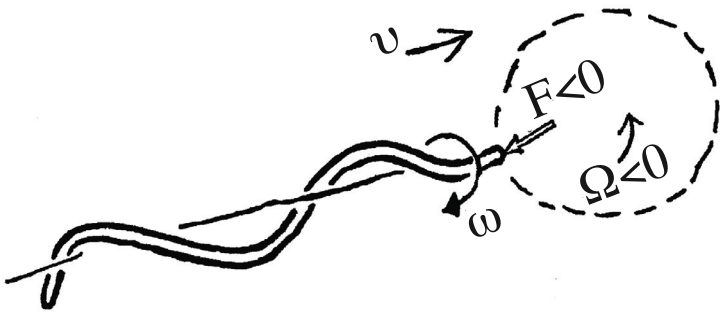

"A propeller in the shape of a right-handed helix connected to a spherical cell, both moving to the right at velocity υ. The propeller and cell rotate in opposite directions, at angular velocities ω and Ω, respectively. The external force F acting on the propeller is directed to the left[2]."

This can be simplified somewhat by removing the bacterial cell from consideration, leaving just the 'propellor', and revealing the combination of force and torque.

"An isolated propeller, subjected to an external force F and an external torque N. It rotates at angular velocity ω and translates at velocity υ[2]."

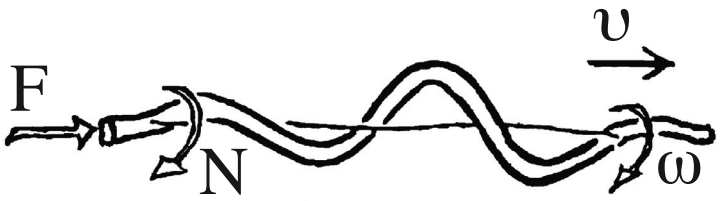

The force and torque are intertwined. This is usually described by a matrix that arises from the formal inter-relations:

$$F = A\upsilon + B\omega$$
$$N = C\upsilon + D\omega$$

That is, both velocity and rotation contribute to both the force and torque.

where the 2 • 2 matrix comprised of the constants (A, B, C and D, all proportional to the viscosity and the size and shape of the 'propellor') is called the propulsion matrix **P**:

$$\mathbf{P} = \begin{bmatrix} A & B \\ C & D \end{bmatrix}$$

[1]1952 (with Felix Bloch) "for their development of new methods for the nuclear magnetic precision measurements and discoveries in connection therewith"

[2]Source: Purcell, EM (1997) The efficiency of propulsion by a rotating flagellum. Proceedings of the National Academy of Science USA 94:11307–11311.

It's important to emphasize that the inter-relations between torque and force (and the propulsion matrix relating the two) are constrained by the low Reynolds number of the bacterial 'universe'. In the context of Newton's laws for translation and rotation, inertia is a dominate force. Not so for the small bacteria as described before. The basic equations –

Pure Translation (fixed direction)		Pure Rotation (fixed axis)	
Position	x	Angular Position	θ
Velocity	$v = dx/dt$	Angular Velocity	$\omega = d\theta/dt$
Acceleration	$a = dv/dt$	Angular Acceleration	$\alpha = d\omega/dt$
Mass	m	Rotational Inertia	I
Second Law	$F_{net}=m\bullet a$	Second Law	$\tau_{net}=I\bullet\alpha$

From Halliday, Resnick and Walker (2005) Fundamentals of Physics 7th edition. John Wiley and Sons. Chapter 10

– must be reconsidered in the context of the viscous drag encountered by the bacteria as it swims. Not only viscous drag on the translational movement, which must be counteracted by constant acceleration. But also viscous drag on the rotating flagella, which generates first the helical shape of the rotating structure, and then, because of the distribution of counteracting forces along the helical flagellar structure caused by frictional drag, the net translational motion of the bacterium.

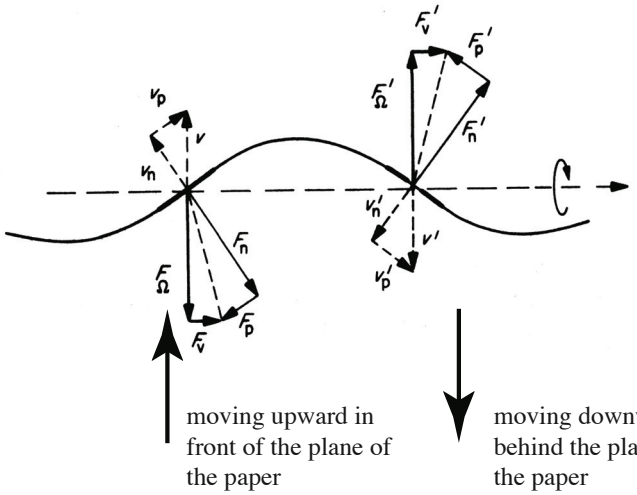

The velocities of each segment (υ) is decomposed into velocities normal (υ_n) and parallel (υ_p) to the segment. The frictional drag forces are also normal (F_n) and parallel (F_p). When F_n and F_p are decomposed into components normal and parallel to the helical axis, the net force F_v, contributes to the forward velocity[1].

Intuitively, it is like turning a corkscrew through a soft material, such that rotation causes the forward motion of translation.

[1]Source: Berg, HC (1993) Random Walks in Biology. Princeton University Press. pp. 79

Both velocity and rotation contribute to both the force and torque.

$$F = A\upsilon + B\omega$$

$$N = C\upsilon + D\omega$$

$$\mathbf{P} = \begin{bmatrix} A & B \\ C & D \end{bmatrix}$$

The constants A, B, C and D (proportional to the viscosity and the size and shape of the 'propellor') comprise the propulsion matrix **P**.

Returning to the analysis by the Nobel Laureate Edward M. Purcell, he performed experiments using large models which were scaled to low Reynolds number by increasing the viscosity of the media. The results are summarized below[1].

Elements of propulsion matrices and propulsion efficiencies for flagellar models dropped in silicon oil

L, cm	L/λ	Pitch angle, °	A, cm	B, cm^2	D, cm^3	ε_{max}, %	f, sec^{-1}
5.2	5	55	0.67	0.032	0.076	0.48	89
7.8	5	39	0.71	0.038	0.06	0.78	85
9.4	5	20	0.74	0.018	0.031	0.34	188
3.1	3	55	0.48	0.023	0.053	0.46	62
7.5	7	56	0.91	0.053	0.13	0.54	100

Test helices of length L, wavelength λ, and specified pitch angle were allowed to sink under their own weight in silicon oil (viscosity ca 1,000 g·cm^{-1}·sec^{-1}). The sinking speeds and speeds of rotation were measured, and A, B, and D were determined and transformed, so that their dimensions are cm, cm^2, and cm^3, respectively. ε_{max} is the maximal propulsion efficiency expected when the test helix is connected to a sphere of radius A. f is the motor speed required to drive that sphere 20A·sec^{-1}.

From a physics viewpoint, efficiencies are independent of 'propellor' shape[1]. The efficiencies are also very low, but in fact, the energy required is low. Purcell calculated energy requirements and obtained a value of 0.5 Watt/kilogram, a small fraction of the bacterial metabolic expenditure[2].

[1]Source: Purcell, EM (1997) The efficiency of propulsion by a rotating flagellum. Proceedings of the National Academy of Science USA 94:11307–11311.

[2]Source: Purcell, EM (1977) Life at low Reynolds number. American Journal of Physics. 45:3–11.

Work Problem:

Purcell calculated low energy requirements for bacterial motility[1], but neglects to say how. Approach this problem from the physics perspective –how much energy is required– and from the biological prespective –how much energy is available to a bacterium under nutrient replete conditions.

Work Problem:

Helical flagella are only one means of propulsion. Would 'jets' work at Low Reynolds Number? Explain.

Work Problem:

Nanotechnological achievements include wonderful microgears and science fiction is replete with nanobots, both good and evil. Are they for real in a Low Reynolds Number World? Explain.

[1]Source: Purcell, EM (1977) Life at low Reynolds number. American Journal of Physics. 45:3–11.

The concept of the Reynolds number came from experiments published by Osborne Reynolds in the 1883: *An Experimental Investigation of the Circumstances which determine whether the Motion of Water shall be Direct or Sinuous, and of the Law of Resistance in Parallel Channels*. in Philosophical Transactions of the Royal Society of London, Vol. 174, pp. 935-982.

In this publication, Reynolds explored the conditions under which the flow of a liquid through a pipe transitioned from smooth laminar flow to turbulent flow. He did this by injecting a stream of dye into the center of a tube through which liquid was flowing (pp. 942):

"When the velocities were sufficiently low, the streak of colour extended in a beautiful straight line through the tube"

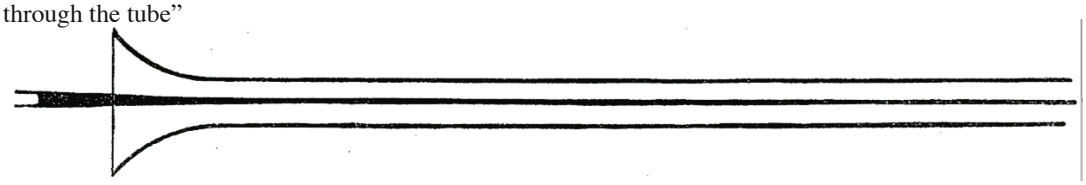

"As the velocity was increased by small stages, at some point in the tube, always at a considerable distance from the trumpet or intake, the colour band would all at once mix up with the surrounding water, and fill the rest of the tube with a mass of coloured water,"

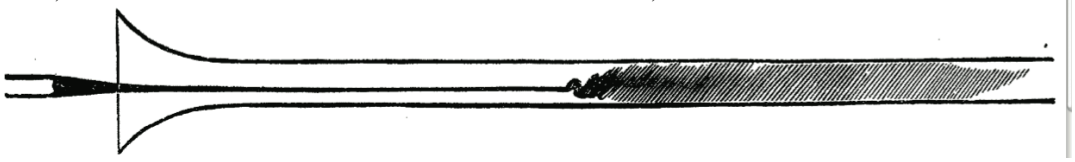

"On viewing the tube by the light of an electric spark, the mass of colour resolved itself into a mass of more or less distinct curls, showing eddies"

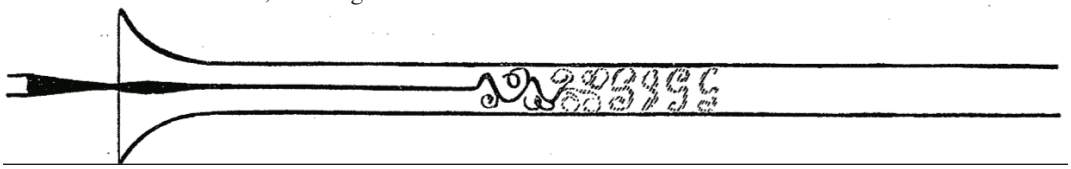

Reynolds presented the following equation (pp. 938):

$$\frac{c\rho U}{\mu}$$

where c is the radus of the tube, ρ is the density, U is the velocity, and μ is the viscosity

stating that "the birth of eddies [should] depend on some definite value of [the equation]". Eventually, the relation became known as the Reynolds Number.

In a recent best-selling book all about the famous bacterial species *Escherichia coli*: **microcosm. e. coli *and the new science of life*** (2009), Carl Zimmer describes the impact that bacteria has had on the Creationist movement, endemic to North America. The creationists, in their latest incarnation as proponents of intelligent design, argue that the complexity of the bacterial flagellar motor precludes the possibility of appearence by evolutionary mechanisms. Instead, it must have been designed:

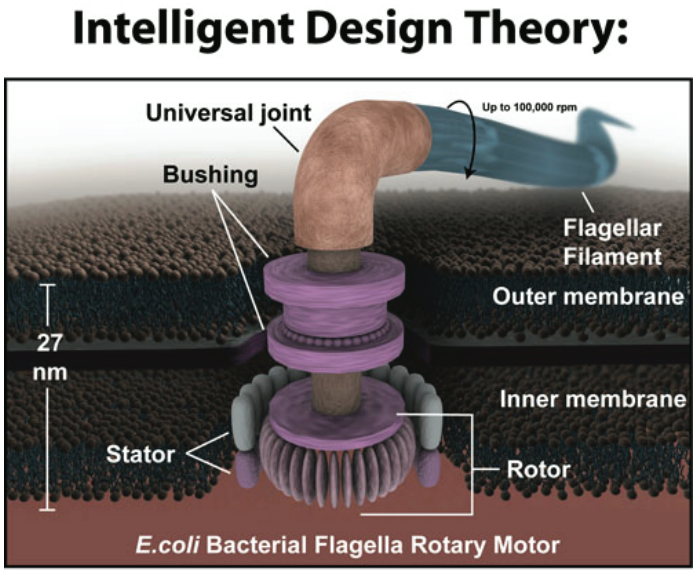

"The sensory and motor mechanism of the E. coli bacterium consists of a number of receptors which initially detect the concentrations of a variety of chemicals. Secondary components extract information from these sensors which in turn is used as input to a gradient sensing mechanism. The output of this mechanism is used to drive a set of constant torque proton-powered reversible rotary motors which transfer their energy through a microscopic drive train and propel helical flagella from 30,000 to 100,000 rpm. This highly integrated system allows the bacterium to migrate at the rate of approximately ten body lengths per second. Would you please find out who filed the patent on this thing?" http://www.cafepress.com/accessresearch/982234

If it looks designed, maybe it is.

There was a court case, brought by parents who did not appreciate the inclusion of intelligent design (with its implied role for God the Engineer) in a science curriculum, the flagellar motor was a key 'witness' during the trial. The judge ruled against the intelligent design proponents, the school board members who had advocated teaching intelligent design in science classrooms were voted out of office.

In fact, the evolution of the flagellar motor has been the focus of much research, especially comparative analysis using phylogenetic techniques, and, surprisingly, explorations of proteins that inject toxins into eukaryotic cells (part of a pernicious strategy used by pathegenic bacteria). The latter appear to be related evolutionarily in two ways: the hollow flagellin protein is similar, as are the structures connecting the bacterial cytoplasm to the external environment.